Geotechnical Aspects of Underground Construction in Soft Ground – Yoo, Park, Kim & Ban (Eds)

A numerical model for the tunnel boring machine interaction with soil

D. Festa, W. Broere & J.W. Bosch
Geo-Engineering Section, Delft University of Technology, Delft, The Netherlands

ABSTRACT: Mechanized shield tunnelling is a reliable way of constructing tunnels in soft soil, particularly in urban areas. However, a lack of understanding of the physical interaction between the TBM-shield, the soil, and the process fluids contributes to the long learning curves often experienced and hinders improvement of the machine's driving rationality. A numerical shield-soil interaction model is proposed that bases the extent and spatial distribution of the displacements induced by the advancing shield on TBM monitoring data. The model includes the unloading-reloading condition of the surrounding soil and the possible infiltration of process fluids around the shield periphery. This infiltration influences the equilibrium of the TBM. A set of novel soil reaction curves is also introduced specifically to model a TBM interaction with the surrounding soil. The study offers an innovative outlook on the tunnelling related soil displacements. Results indicate that a more rational approach to mechanized shield tunnelling in soft soil is possible.

1 INTRODUCTION

Tunnel Boring Machines (TBMs), used to construct tunnels in increasingly challenging and built-up environments, have nowadays few technically and economically viable alternatives. However, as conditions become more difficult, also stricter standards are set in order to minimize the disruption due to tunnelling. This urges research on improving the understanding of the physics governing the interaction between the TBM and the soil.

Mechanised tunnel construction can be subdivided in excavation and support of the front, temporary support of the surrounding soil, response of the lining to the soil weight, and tail-void grout mortar consolidation. Effect at the face and tail have been studied in detail. This paper focuses on the temporary support of the surrounding soil by the TBM-shield.

A numerical model is introduced to describe the static equilibrium of the TBM during advance, given that the forces and moments are balanced. The driving forces applied to advance and steer the shield (active forces), are balanced by external reactions exerted by the surrounding soil (passive forces). The reaction of the surrounding soil depends upon the characteristics of the soil and its stress-strain history. Tunnelling-induced stress-strain changes are determined by the sequence of construction process, mainly the specific driving pattern of the TBM-shield within the cavity excavated at its front, hereafter named excavation profile.

The exact shape of the excavation profile and the position and orientation of the shield within it are determined at every advance stage through a shield kinematic model (Festa et al. 2011, 2014a) and from there the amount of soil compression and relaxation at the shield-soil interface is quantified. These interface displacements are processed via a soil reaction model providing the soil stress distribution at the shield periphery. Combined with the driving actions the shield equilibrium is evaluated.

This paper describes the soil reaction model adopted for the static analysis and the analysis results. The soil reaction model captures the non-linearity of the soil and its response in case of loading-reloading and is based on FEM analyses, subsequently approximated by analytic expressions The combined static equilibrium shows the extent to which the model can describe the physical processing around the shield. Finally, the influence on the shield equilibrium of the tail-void grouting is discussed.

Input for the model is TBM and soil displacement monitoring data collected during the construction of the Hubertus Tunnel, a double-tube road tunnel in The Hague, NL, excavated through Pleistocene sand by means of a 10.235 m long slurry shield. The active forces derived from the TBM monitoring data are presented in Festa et al. (2012). The correlation between the modelled shield-soil interface displacements and the observed soil displacements is investigated in Festa et al. (2013, 2014b).

2 SOIL REACTION MODEL

As most soils exhibit a non-linear stress-strain response dependent on the deformation history, simplified soil-reaction models such as the Mohr-Coulomb linear elastic-perfectly plastic one can lead

to poor estimates of the stresses at the shield-soil interface. A more realistic soil reaction is needed.

Analytical and numerical soil models can both serve that purpose and both offer advantages when simplifications are introduced. For instance, the analytical approach may have a closed from solution, but significant simplifications are needed. Numerical methods, although more flexible, need a larger computation effort for each combination of boundary conditions. Alternative solutions proposed in literature are based on simplified soil reaction curves with cut-offs based on the concepts of active and passive stress states (Sugimoto & Sramoon 2002). The dependency of such curves on the radial position around the tunnel is an interesting aspect. Unfortunately these computationally advantageous models do not consider the dependency of the soil stiffness on the actual stress level and disregard the unloading-reloading response. Neither do they account for the fact that the soil mass above the tunnel is more limited than underneath. These aspects are faced in the newly proposed model.

2.1 *New soil reaction curves*

Novel soil reaction curves are proposed to model the problem of a circular cavity undergoing concentric displacements. This model disregards ovalisation and buoyancy and assumes 2D axially-symmetric displacements. These simplifications were accepted after observing the modest rate of change of the interface displacements in longitudinal and radial direction.

The soil reaction curves are interpolated from soil response curves from PLAXIS 2D 2012 FEM analyses for a range of initial stress states and deformation patterns. A circular cavity with the radius of the TBM-shield was located at −15, −20, and −25 m. This cavity, lined with a very stiff but weightless ring, was cyclically expanded and contracted and the stress-displacement relations at representative locations around the tunnel were recorded.

The loading-unloading case consists of an expansion of 1.5% followed by an equal contraction, corresponding to a radial change of about 40 mm and the unloading-reloading case the exact opposite. Equal expansion and contraction restores the initial lining position at the end of the loading cycle.

Converting the FEM results into an analytical fit facilitates a simplified numerical model replacing more accurate but complex FE calculations at every advance step. The explicit analytical expressions can be directly applied to the calculated deformation history of each of the 50×180 regions in which the shield periphery has been discretized for the kinematic analysis, providing an approximated but quick response.

In the 50×100 m FE model the Hardening Soil constitutive model, drained conditions, and groundwater table at ground level are applied, with parameters in Table 1 as derived from the Geotechnical Report of the Hubertus Tunnel (TEC 2004). E_{ur}^{ref} has been set at $3E_{50}^{ref}$, in accordance with the PLAXIS 2D (2012) Material Models Manual.

Table 1. Soil parameters FE model.

Parameter	Unit	Value
Material model	—	Hardening Soil
γ_{unsat}	[kN/m^3]	17
γ_{sat}	kN/m^3]	20
E_{50}^{ref}	kN/m^3]	$40{\cdot}10^3$
E_{oed}^{ref}	kN/m^3]	$40{\cdot}10^3$
E_{ur}^{ref}	kN/m^3]	$120{\cdot}10^3$
φ' (phi)	[°]	32
ψ (psi)	[°]	2
c'_{ref}	kN/m^3	0

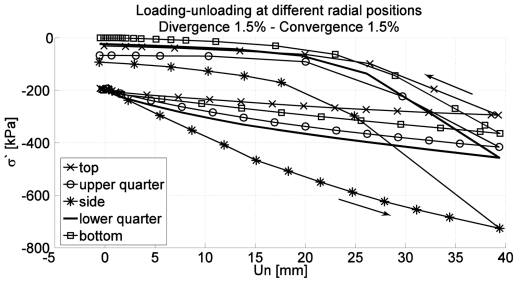

Figure 1. Expansion-contraction as from FE model. Top, upper quarter, side, lower quarter, and bottom correspond to 180°, 135°, 90°, 45°, and 0°, counter-clockwise and from bottom.

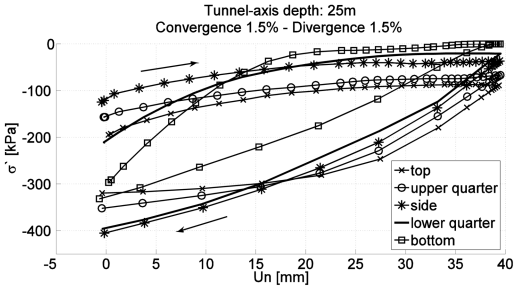

Figure 2. Contraction-expansion as from FE model. Top, upper quarter, side, lower quarter, and bottom correspond to 180°, 135°, 90°, 45°, and 0°, counter-clockwise and from bottom.

Figures 1 and 2 show some results of the FE analyses. Figure 1 highlights the dependency of the soil stiffness with the radial direction. Figure 2 shows the combined effect on the soil stiffness of radial orientation and initial stress.

2.2 *Analytical formulation*

Equation 1 links radial expansion and normal stress

$$\sigma_L^{ref} = a_L \cdot (x + x_0)^{b_L} \quad (1)$$

x stands for the radial increase (in mm) and σ_L^{ref} for the normal stress (in kPa). The formula is calibrated on an initial normal effective stress $p_{ref} = -200$ kPa and $x_0 = 4$ mm. The subscript L indicates that loading is considered. a_L and b_L are calibration parameters that account for the dependency on the radial position around the shield ϑ

$$\vartheta \leq \frac{\pi}{2} \qquad \begin{cases} a_L = a_3 + a_1 \cdot \sin^{a_2} \vartheta \\ b_L = b_3 + b_1 \cdot \sin^{b_2} \vartheta \\ c_L = Re(c_1 - c_2 \cdot \cos^{c_3} 2\vartheta) \end{cases} \tag{2}$$

$$\frac{\pi}{2} < \vartheta \leq \pi \qquad \begin{cases} a_L = a_6 + a_4 \cdot \sin^{a_5} \vartheta \\ b_L = b_6 + b_4 \cdot \sin^{b_5} \vartheta \\ c_L = Re(c_4 - c_5 \cdot \cos^{c_6} 2\vartheta) \end{cases} \tag{3}$$

$$\begin{aligned} A &= [51.96, 4.4, -134.2, 71.3, 2.1, -153.5] \\ B &= [0.33, 3.7, 0.26, 0.41, 2.7, 0.17] \\ C &= [2, -2, 1 + 0.14\mathrm{i}, 2, -3, 1 + 0.27\mathrm{i}] \end{aligned} \tag{4}$$

Eq. 1 is generalized for the initial stress level p_0. Differentials are indicated with the independent variable as subscript:

$$\sigma_{L,x}^{ref} = a_L \cdot b_L \cdot (x + x_0)^{b_L - 1} \tag{5}$$

and, at the generic initial stress p_0,

$$\sigma_{L,x(x=0)} = \sigma_{L,x(x=0)}^{ref} \cdot \frac{p_0}{p_{ref}} \tag{6}$$

The load curve at p_0 is obtained by successive increments according to an explicit integration scheme

$$\sigma_L^i = \sigma_L^{i-1} + \sigma_{L,x}^{i-1} \cdot \left(x^i - x^{i-1}\right) \tag{7}$$

in which the generic first derivative is

$$\sigma_{L,x} = \sigma_{L,x(x=0)} \cdot \left(\frac{\sigma_L}{p_0}\right)^{-c_L} \tag{8}$$

The radial contraction and the normal stress following a previous expansion is

$$\sigma_U^{ref} = a_U + b_U \cdot (x)^{c_U} \tag{9}$$

in which x is the radial contraction (in mm) and σ_U^{ref} the normal stress (in kPa). Eq. 9 describes unloading after a previous expansion of 50 mm at an initial stress $p_{ref} = -200$ kPa. a_U, b_U, and c_U are calibration parameters. As for the loading arm, Eq. 9 is adjusted to describe generic initial stress and deformation.

Similar analytical expressions used for the unloading-reloading case are omitted here for brevity.

The proposed formulation is compared with the curves from the FE model and, based on the Figures 3 and 4 judged satisfactory.

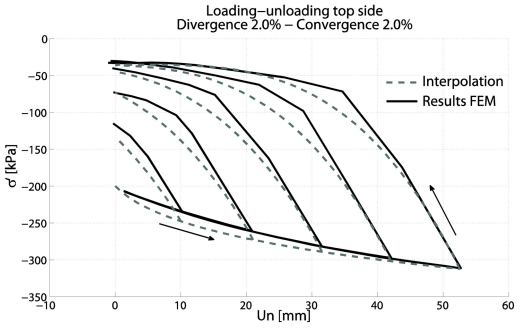

Figure 3. Loading-unloading for multiple deformation stages. Solid lines: FEM results. Dashed lines: interpolated values as from the analytical expressions.

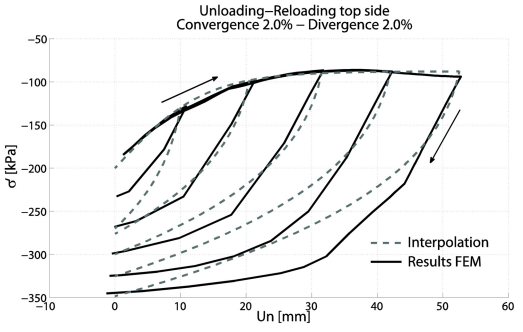

Figure 4. Unloading-reloading for multiple deformation stages. Solid lines: FEM results. Dashed lines: interpolated values as from the analytical expressions.

3 MECHANICAL EQUILIBRIUM

The global equilibrium of forces and moments must be satisfied in every direction, and is verified in three directions, the first coincident with the TBM axis (longitudinal component), the second transversal to it in horizontal direction (transversal component), and the third aligned with the Earth's gravity (vertical component).

Model results show that equilibrium is only achieved for certain locations and the physics of the shield-soil interaction are not fully captured by the model. For example Figure 5 shows the transversal equilibrium over the sector $-820 \div -780$ m, which shows a force imbalance in the order of 16% of the thrust force It is believed that grout mortar infiltration around the shield may play a crucial part in explaining this imbalance.

Figures 6 and 7 show the distribution of the total normal stresses on the TBM without and with the grout infiltration, respectively. When the grout infiltrates the void between the shield and the soil, higher normal stresses originate in the infiltrated sectors. The redistribution of the normal stresses affects the horizontal equilibrium. When infiltrating grout is not included, the calculated imbalance amounts to -10.27 MN leftward. When grout infiltration is considered, the

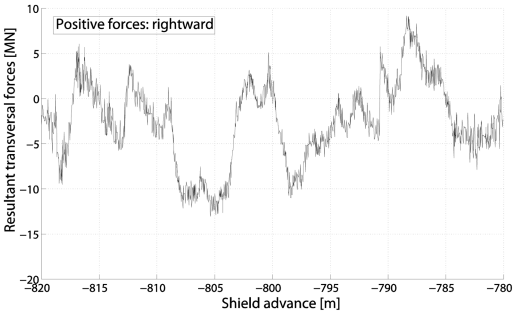

Figure 5. Resultant transversal forces – sector $-820 \div -780$ m (grout infiltration not taken into account).

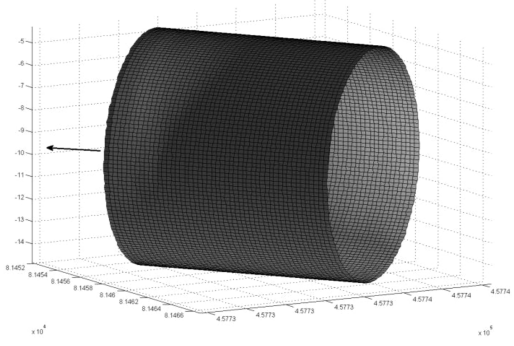

Figure 6. Total normal stress distribution without grout infiltration. Advance -806.328 m south alignment. Left-hand side. Grayscale calibration: white = 700 kPa; black: 0 kPa.

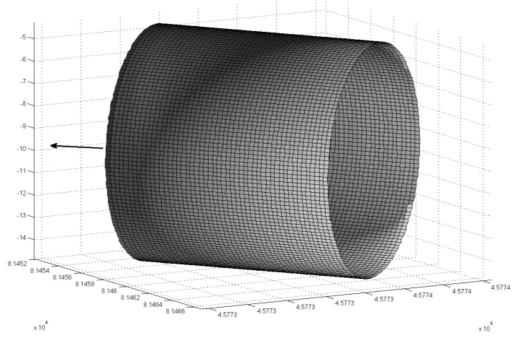

Figure 7. Total normal stress distribution with grout infiltration. Advance -806.328 m south alignment. Left-hand side. Grayscale calibration: white = 700 kPa; black: 0 kPa.

imbalance changes to a rightward $+4.14$ MN. The transversal force induced by the infiltrating grout proves of the same order as the imbalance in the simplified model without grout effect. This shows that grout infiltration around the shield influences the equilibrium of the TBM.

4 CONCLUSIONS

The proposed numerical method for the equilibrium of a TBM-shield sheds new light on stresses and deformations at the shield-soil interface during advance. The stresses on the shield are modelled using novel soil reaction curves.

The results from static equilibrium calculations show both the potential and limits of the model. Decent equilibrium is found at several intervals. In contrast, at other locations the calculated equilibrium is poor and model improvements are required.

The presence of grout in the void around the shield skin can yield the required missing force. At several of the locations where the simplified kinematic model did not achieve static equilibrium, the tail-void grout can provide the required force when it infiltrates in the void between the shield periphery and the surrounding soil where the contact stress is sufficiently low. This is an indication that forward flow of tail void grout may well occur in practice.

Refinement of the proposed model and verifications based on physical models are recommended.

REFERENCES

Festa, D. et al. 2011. Tunnel-boring process in soft soils: improved modelling for reliability enhancement. Kinematic behaviour and tail grouting monitoring. *Proceedings WTC-2011 Underground spaces in the service of a sustainable society*, Helsinki, 20–26 May

Festa, D., Broere, W., Bosch, J.W. 2012. An investigation into the forces acting on a TBM during driving – Mining the TBM logged data. *Tunnelling and Underground Space Technology* (32): 143–157

Festa, D. et al., 2013. Tunnelling in soft soil: Tunnel Boring Machine operation and soil response. *International Symposium on Tunnelling and Underground Space Construction for Sustainable Development*, Seoul, Korean Tunnelling and Underground Space Association, 18–20 March

Festa, D., Broere, W., Bosch, J.W. 2014a. Kinematic behaviour of a Tunnel Boring Machine in soft soil: theory and observations, *Tunnelling and Underground Space Technology (under review)*

Festa, D., Broere, W., Bosch, J.W. 2014b. Correlation between the kinematics of a Tunnel Boring Machine and the observed soil displacements, *Tunnelling and Underground Space Technology (under review)*

Sugimoto, M. & Sramoon, A. 2002. Theoretical model of shield behavior during excavation. I: Theory. *J. Geotech. Geoenviron. Eng.*, 128(2): 138–155

TEC Tunnel Engineering Consultants 2004. Hubertustunnel Geotechnisch Basis Rapport